Proc. Natl. Acad. Sci. USA
Vol. 85, pp. 5703–5707, August 1988
Medical Sciences

Electron paramagnetic resonance measurements of free radicals in the intact beating heart: A technique for detection and characterization of free radicals in whole biological tissues

(*in vivo* electron paramagnetic resonance/loop-gap resonator/free radical metabolism/oximetry/reperfusion)

JAY L. ZWEIER* AND PERIANNAN KUPPUSAMY

The Electron Paramagnetic Resonance Laboratories, Department of Medicine, Cardiology Division, The Johns Hopkins Medical Institutions, Baltimore, MD 21224

Communicated by William A. Hagins, April 25, 1988 (received for review March 18, 1988)

ABSTRACT **Free radicals have been hypothesized to be important mediators of disease in a variety of organs and tissues. Electron paramagnetic resonance (EPR) spectroscopy can be applied to directly measure free radicals; however, it has not been possible to measure important biological radicals *in situ* because conventional spectrometer designs are not suitable for the performance of measurements on whole organs or tissues. We report the development of an EPR spectrometer designed for optimum performance in measuring free radicals in intact biological organs or tissues. This spectrometer consists of a 1- to 2-GHz microwave bridge with the source locked to the resonant frequency of a recessed gap loop-gap resonator. With this spectrometer, radical concentrations as low as 0.4 μM can be measured. Isolated beating hearts were studied in which simultaneous real time measurements of free radicals and cardiac contractile function were performed. This *in vivo* EPR technique was applied to study the kinetics of free radical uptake and metabolism in normally perfused and globally ischemic hearts. In addition, we show that this technique can be used to noninvasively measure tissue oxygen consumption. Thus, it is demonstrated that EPR spectroscopy can be applied to directly measure *in vivo* free radical metabolism and tissue oxygen consumption. This technique offers great promise in the study of *in vivo* free radical generation and the effects of this radical generation on whole biological tissues.**

Electron paramagnetic resonance (EPR) spectroscopy was developed in the late 1940s. Advances in microwave source and signal processing technology enabled the development of instrumentation capable of performing sensitive measurements of free radicals and paramagnetic ions in solids and small chemical samples. Since that time, EPR spectroscopy has become an important technique for studying the many chemical reaction mechanisms involving free radical intermediates. Over the past decade, free radicals have been recognized to be important mediators of a large variety of clinical disease processes including heart attack, stroke, respiratory distress syndrome, acute tubular necrosis of the kidney, reperfusion injury of a variety of organs, and oncogenesis and tumor promotion (1, 2). Even the process of aging has been proposed to be secondary to the formation of reactive oxygen free radicals (3). Thus, free radicals are thought to mediate many of the most prevalent diseases causing morbidity and mortality in the United States today.

EPR spectroscopy has been widely applied to study biological and biochemical problems of isolated proteins and enzymes involving free radicals and paramagnetic metal ions; however, similar measurements have not been made in intact biological tissues. Conventional spectrometer designs that are commercially available are typically built with microwave frequencies of 8–10 GHz (X-band) or 35–40 GHz (Q-band) with standard rectangular or cylindrical resonant cavities. With these spectrometer designs, the maximum thickness of the nonfrozen aqueous sample that can be studied is approximately 1 or 0.2 mm, respectively.

We report the development of an EPR spectrometer designed to enable high sensitivity EPR measurements of whole biological organs and tissues. Using this spectrometer, we measure physiologic (μM) concentrations of free radicals in the intact beating heart. This technique provides nondestructive measurements of the kinetics of free radical uptake and metabolism in the intact beating heart. Simultaneous measurements of cardiac contractile function and free radical concentrations were performed, enabling direct real time correlation of the effects of free radicals on heart function. In addition, this *in vivo* EPR technique was applied to noninvasively measure other important tissue properties including tissue oxygen consumption.

METHODS

Lumped circuit resonator designs were described as early as 1940 and recently these resonators have been demonstrated to be useful for application to NMR and EPR spectroscopy (4, 5). These designs were referred to initially as split-ring resonators and subsequently the term loop-gap resonator has been coined to encompass a broad range of variations of these designs (5). The split-ring resonator or loop-gap resonator designs can be visualized as a split conducting cylinder with an inductive ring, or loop, and two air gap plate capacitors (Fig. 1). The critical dimensions of this resonator include r, the resonator radius; t, the gap size; w, the width of the capacitive plates; n, the number of gaps; z, the resonator length. This resonator is placed within a conducting shield of radius R, which must be less than the cutoff wavelength for the lowest excited propagational mode of cylindrical waveguide to suppress the external radiation of microwave energy observed when the resonator dimensions approach quarter wavelength. Coupling of microwave power is achieved via an inductive coupling loop. The resonance frequency, ν, of this resonator is defined by the equation

$$\nu = \frac{1}{2\pi r}\left(1 + \frac{r^2}{R^2 - (r + w)^2}\right)^{1/2}\left(\frac{nt}{\pi w \varepsilon \mu_o}\right)^{1/2} \times \left(\frac{1}{1 + 2.5(t/w)}\right)^{1/2}, \quad [1]$$

The publication costs of this article were defrayed in part by page charge payment. This article must therefore be hereby marked "*advertisement*" in accordance with 18 U.S.C. §1734 solely to indicate this fact.

Abbreviations: EPR, electron paramagnetic resonance; TEMPO, 2,2,6,6-tetramethylpiperidinyloxy radical.

*To whom reprint requests should be addressed at: Division of Cardiology, Francis Scott Key Medical Center, Building B1 South, 4940 Eastern Avenue, Baltimore, MD 21224.

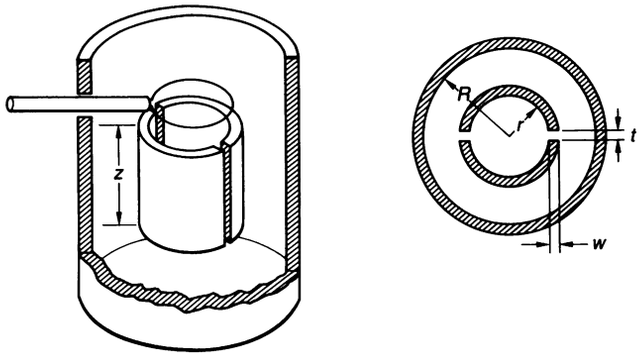

FIG. 1. Diagram of the loop-gap resonator.

and the Q is defined by the equation

$$Q = \frac{r}{\delta} \frac{\left(1 + \frac{r^2}{R^2 - (r+w)^2}\right)}{\left[1 + \left(1 + \frac{w}{r} + \frac{R}{r}\right)\left(\frac{r^2}{R^2 - (r+w)^2}\right)^2\right]}, \quad [2]$$

where $\delta = (1/\pi\mu_o\nu\sigma)^{1/2}$, ε is the dielectric constant, μ_o is the susceptibility, and σ is the conductivity.

Loop-gap resonators are superior to conventional cavity resonators for accommodating large aqueous samples based on the fact that the maximum **E** field is localized within the gap and the maximum **H** field is localized in the bore. Thus, maximum **H** field and minimum **E** are observed at a sample in the center of the resonator bore minimizing the loss in resonator Q observed from loading with a lossy dielectric aqueous sample. Therefore, relatively high Q values can be observed in the presence of high filling factors, which enables high sensitivity to be obtained in EPR applications. The maximum attainable sensitivity for EPR measurements at any given frequency is defined by the equation (6, 7)

$$c_{min} = K/Q_u\eta\omega_o^2(P_w)^{1/2}, \quad [3]$$

where c_{min} is the minimum detectable radical concentration, Q_u is the unloaded Q of the resonator, η is the filling factor, ω_o is the microwave frequency, P_w is the applied microwave power, and K is a frequency-independent constant. Thus, maximum sensitivity is obtained when the filling factor, the Q, and the resonance frequency are maximized.

The magnitude of **E** fringe fields extending outside the gap into the resonator bore increases as the ratio t/w increases. Therefore, we observe that t/w should be <0.2.

From the equations for ν and Q theoretical predictions of resonator dimensions yielding optimum Q were performed. These predictions were then experimentally tested. A rugged versatile resonator design was constructed suitable for *in vivo* tissue EPR applications. As shown in Fig. 2, this resonator design consisted of an outer shield (R = 2.06 cm), an inner loop gap resonator insert rod, the resonator halves that attach to the insert rod, a coupling loop, and a mechanical micrometer controlled stage used to precisely move the resonator with respect to the coupling loop. The shield was machined from rexolyte plastic blocks and a series of resonator inserts and resonator halves were also machined from rexolyte. The shield was silvered with a 10-μm thickness of silver deposited by ion beam deposition. The resonator halves were coated with pure 99.9% silver foil, which was attached to the plastic with transfer adhesive. For optimum performance in EPR applications with maximum Q, the silvered conducting surface of the resonator must be at least 10 times the microwave frequency skin depth; however, to achieve adequate field modulation penetration at frequencies of 50 or 100 kHz, the thickness cannot exceed 25–50 μm. Therefore, the resonator was silvered with foil 25 μm thick. The coupling loop consisted of a short length of 3-mm-diameter semirigid coax with inner conductor looped and soldered to the outer conductor. Coupling of microwave power was varied by moving the resonator with respect to the coupling loop with precise movement achieved by using the micrometer controlled stage. A series of 400 resonators were built and tested with various dimensions of r, t, w, and n. To accommodate aqueous sample sizes as large as 10–20 mm diameter, the resonant frequency must be in the range of 1–2 GHz, L-band, or below. It was observed that the experimentally measured resonance frequencies matched the theoretically predicted values to within 5% accuracy; however, significant deviations in the measured Q values were observed. An optimum (filling factor $\times$ Q) product was observed for aqueous samples of 13–15 mm diameter with resonator dimensions r = 13 mm, t = 0.25 mm, w = 3 mm, n = 2, and z = 25 mm. The resonant frequency of this resonator was 1.1 GHz with an unloaded Q of 2000 and a Q of 600 when the resonator was filled with a 13-mm aqueous sample. It was observed that the Q of the sample containing resonator could be further increased by recessing the gaps with semicylindrical holes (Fig. 3). Recessing the gaps has the effect of decreasing **E** fringe field at the sample, decreasing dielectric loss, and increasing resonator Q with only a small effective decrease in resonator filling factor. The recessed loop-gap resonator with dimensions r = 13 mm, t = 0.25 mm, w = 3 mm, n = 2, z = 25 mm, and recession radius a = 4 mm had a resonant frequency of 1.1 GHz, with a Q of 1000 when loaded with a 13-mm-diameter aqueous sample. Field modulation was achieved with 8-cm-diameter 100-turn modulation coils mounted on the side walls of the resonator shield. The modu-

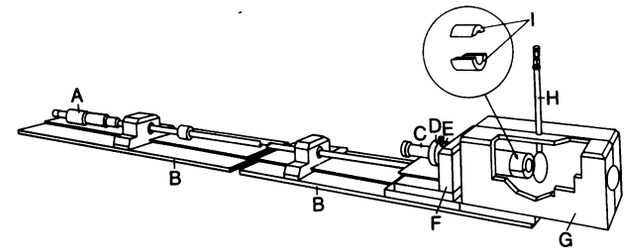

FIG. 2. Diagram of the loop-gap resonator design used for studies of intact biological tissues. A, coupling adjustment micrometer; B, support rail; C, sample tube; D, sample tube holder; E, resonator support rod; F, spring-loaded resonator coupling adjustment stage; G, shield; H, semirigid coax coupling loop; I, resonator halves. The outer shield, G, is shown partially peeled open to illustrate the resonator and coupling loop within.

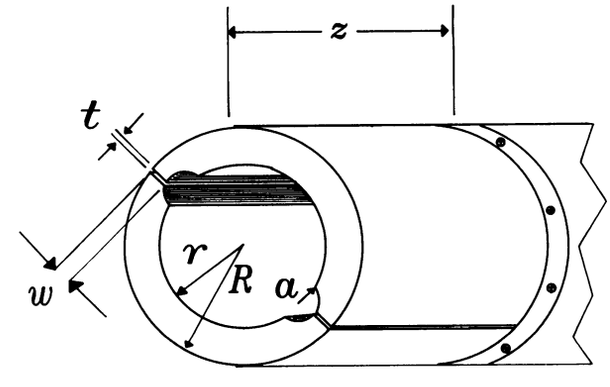

FIG. 3. Diagram of the recessed loop-gap resonator used in the studies of intact hearts. Gaps are recessed by a semicylindrical hole of radius a.

lation amplitude and signal phase were calibrated with a point sample of the diphenylpicrylhydrazyl radical.

Resonators were tested with an EIP 931 or Wavetek 2005 microwave sweeper. Measurements of resonant frequency, Q, and H_1 fields were performed. Unloaded Q was measured as twice the resonance width at half-power absorption with the resonator critically coupled. H_1 field values were measured with a copper sphere as described (8).

EPR spectra were obtained at L-band, 1–2 GHz, using a specially designed microwave bridge containing a cavity stabilized transistor oscillator as the frequency source, a directional coupler with a test port connected to a frequency counter, a variable attenuator with a 60-dB range, a three-port circulator, a shotkey diode detector, and a preamplifier stage with output connected to the input of the signal channel lock-in amplifier. The oscillator had a maximum power output of ≈100 mW and was locked to the resonant frequency of the sample resonator with an AFC feedback loop.

Isolated rat hearts were perfused by the method of Langendorff at 37°C with a Krebs bicarbonate-buffered perfusate consisting of 117 mM NaCl, 24.6 mM $NaHCO_3$, 5.9 mM KCl, 1.2 mM $MgCl_2$, 2.0 mM $CaCl_2$, 16.7 mM glucose, bubbled with 95% O_2/5% CO_2 as described (9).

RESULTS

Evaluation of Sensitivity. Studies were performed to evaluate the sensitivity of the spectrometer for performing EPR measurements on free radicals in large aqueous samples. Sample tubes of 13 and 15 mm were studied with sample volumes of 1–2 ml. As shown in Fig. 4, spectrum A, with 2-min spectral acquisitions, signal/noise ratios of >1200 were obtained on 1.0 mM solutions of 2,2,6,6-tetramethylpiperidinyloxy radical (TEMPO); with a radical concentration of only 2 μM, a signal/noise ratio >5 was observed (Fig. 4, spectrum B). Thus, free radical concentrations as low as 0.4 μM were detectable.

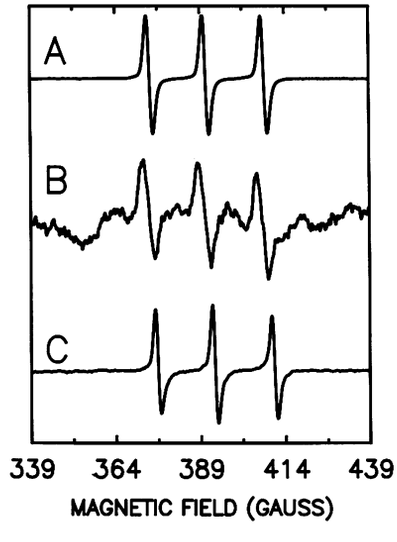

FIG. 4. Spectrum A, EPR spectrum of an aqueous 1.0 mM TEMPO solution filling a 13-mm cylindrical tube. The resonant frequency is 1.085 GHz with a modulation amplitude of 0.5 G, modulation frequency of 50 kHz, microwave power of 100 mW, and acquisition time of 2 min. Spectrum B, EPR spectrum of an aqueous 2 μM TEMPO solution filling a 13-mm cylindrical tube. The spectrum was acquired as described for Spectrum A. Spectrum C, EPR spectrum of a perfused rat heart in a 13-mm tube. The heart was perfused with a solution containing 1.0 mM TEMPO. A 2-min acquisition was performed 5 min after starting the radical infusion. This spectrum was obtained as described for spectrum A, except that the resonant frequency was 1.095 GHz.

Radical Uptake and Clearance in the Perfused Heart. Hearts were removed from rats (200 g) and perfused in a Langendorff mode with a constant coronary flow of 10 ml/min, yielding a perfusion pressure of ≈80 mmHg. A left ventricular balloon was inserted from the left atrium to the left ventricle to enable continuous measurement of left ventricular pressures and heart rate. The hearts were inserted into 13-mm tubes and the tube placed within the resonator (Fig. 5). A drainage catheter was inserted at the bottom of the tube and connected to an aspiration pump to remove effluent perfusate preventing flooding of the resonator. Removal of perfusate solution from around the heart resulted in higher resonator Q values and higher sensitivity EPR measurements. In addition, removal of all effluent perfusate enabled measurements of radical uptake and clearance from the heart, eliminating the problem of an effluent perfusate signal. The microwave bridge AFC loop functioned to minimize the frequency noise that resulted from the motion of the beating heart.

Control spectra were recorded and then an infusion of the TEMPO free radical was started with a concentration of 1.0 mM in the perfusate solution. Repetitive 2-min EPR acquisitions were then performed for 30 min. Infusion of the radical was then stopped and repetitive 2-min spectra were acquired to measure the kinetics of radical clearance. The left ventricular developed pressure of these hearts was ≈120 mmHg with a fixed diastolic pressure of 12 mmHg and an intrinsic heart rate of 200–250 beats per min. Infusion of the radical-containing perfusate had no effect on contractile function or heart rate. Prior to infusion of the TEMPO radical, no EPR signal was observed. Immediately after the start of the infusion, however, the prominent triplet TEMPO signal was clearly seen with good signal/noise ratios of >400 (Fig. 4, spectrum C). The intensity of the signal increased rapidly over the first 5 min of infusion with a half maximum after 2 min, followed by a further gradual increase over the next 10 min of administration.

To get an understanding of the nature and rate of radical clearance and uptake we performed a nonlinear (exponential) least-squares fitting of the observed intensity data to functions of the form $I = I_0\exp(-kt)$ or $I = I_0[1 - \exp(-kt)]$, respectively, using standard fitting routines. As shown in Fig. 6 the time course of radical uptake could be precisely modeled as a first-order exponential process with a rate constant $k = 0.85 \pm 0.05$ min^{-1}.

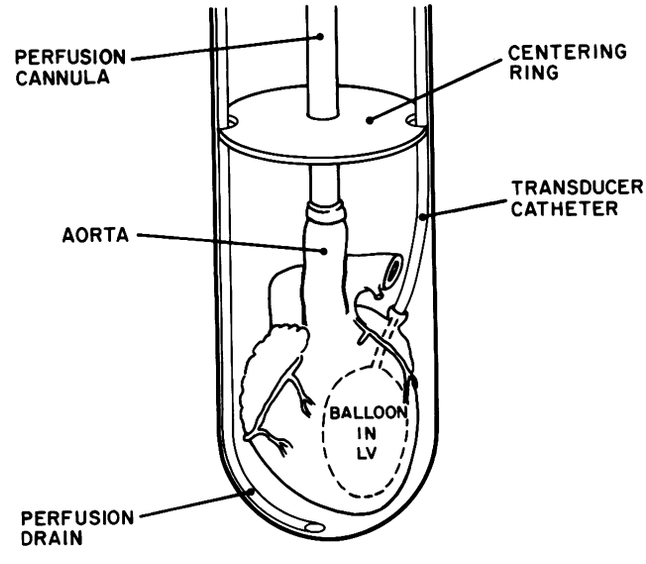

FIG. 5. Diagram of perfused heart preparation.

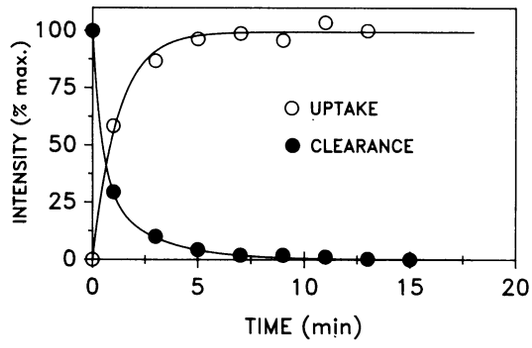

FIG. 6. Graph of kinetics of radical uptake (○) and clearance (●) in the isolated perfused heart. For measurements of radical uptake, hearts were perfused with 1.0 mM TEMPO starting at time 0 and repetitive 2-min EPR acquisitions of 100-G sweeps were performed. The signal intensity was determined from double integration of the signal. Kinetic data were fit with a single exponential with rate constant $k = 0.85\ min^{-1}$. For measurements of radical clearance, radical infusion was stopped after 30 min at time 0 and repetitive 2-min acquisitions were performed. The process of radical clearance required fitting with a linear combination of 2 exponentials, one with rate constant $k = 2.2\ min^{-1}$ with a weight of 65% and the other with rate constant $k = 0.4\ min^{-1}$ with a weight of 35%.

Clearance of the radical from the heart after termination of infusion was observed to proceed in more than a single phase. A single exponential function was not sufficient to fit the observed data satisfactorily. A plot of log(intensity) vs. time showed clearly the involvement of two processes (Fig. 7 *Inset*). Therefore, the data were fitted with a linear combination of two exponentials, which yielded the rate constants for the two processes as $2.2 \pm 0.2\ min^{-1}$ and $0.40 \pm 0.04\ min^{-1}$. The faster process accounted for ≈65% of the radical loss, probably representing the vascular washout, while the slower process, which accounted for 35% of the loss, may be due to cellular enzyme reduction.

Measurement of Radical Metabolism in the Ischemic Heart. Hearts were perfused with 1.0 mM TEMPO as described above for 30 min and then subjected to global ischemia with perfusion stopped. Repetitive 2-min EPR acquisitions were then performed for 30 min. A gradual decrease in radical concentrations was observed that could be precisely fit with a single first-order exponential with a rate constant of $0.40 \pm 0.01\ min^{-1}$ (Fig. 7). This observed rate constant was identical to that of the slower process observed during radical clearance of the normally perfused heart.

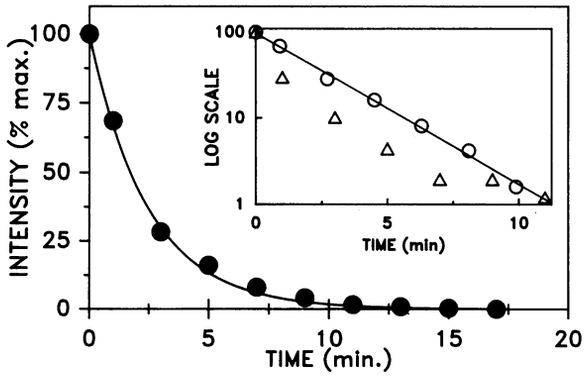

FIG. 7. Graph of kinetics of free radical metabolism in the ischemic heart. The heart was loaded with a 30-min infusion of 1.0 mM TEMPO followed by induction of ischemia at time 0. Measurements were performed as described in Fig. 5. Kinetic data of radical decay were fit with a single exponential with rate constant $k = 0.40\ min^{-1}$. (*Inset*) Semilogarithmic plot of radical decay (○) is linear. Also shown, for comparison, are decay data of the perfused heart (△), which is nonlinear and required two exponential functions for fitting.

Measurement of Myocardial Oxygen Consumption. Molecular oxygen is the only component in air that is paramagnetic and it exists in the triplet ground state with a spin $S = 1$. In solution, it can undergo Heisenberg exchange interaction with other paramagnetic species, such as the spin label TEMPO. This exchange interaction will result in a broadening of the observed EPR line. The magnitude of this broadening depends on the exchange rate, ω, which in turn is governed by Smoluchowski equation

$$\omega = 4\pi R\{D(O_2) + D(\text{TEMPO})\}[O_2], \quad [4]$$

where R is the interaction distance between oxygen and the spin label, which is generally assumed to be 4.5 Å, $D(O_2)$ and D(TEMPO) are, respectively, the diffusion constants of oxygen and TEMPO, and $[O_2]$ is the concentration of oxygen. Normally in aqueous solutions D(TEMPO) is much smaller compared to $D(O_2)$ and so it can be omitted. The exchange rate ω is related to the observed peak to peak width of a Lorentzian EPR derivative line, $H_{p\text{-}p}$, as

$$\omega = (\sqrt{3}/2)\gamma H_{p\text{-}p}, \quad [5]$$

where γ is the gyromagnetic ratio. Combining Eqs. 4 and 5

$$H_{p\text{-}p} = (8\pi R/\gamma\sqrt{3})D(O_2)[O_2]. \quad [6]$$

Thus, one can compute the $[O_2]$ from the measured EPR line width changes, ΔH.

In our experiments, we carefully measured the line width in normally perfused hearts and the line width changes observed during ischemia. During normal perfusion the line width remained invariant at 1.73 ± 0.02 G. This value did not change during the washout of the spin label, even when the spin label concentration decreased by a factor of 10. However, after the induction of ischemia, the width of the line gradually decreased and the line continued to sharpen with increasing duration of ischemia. This is in accordance with the decrease in oxygen concentration that would be expected to occur in ischemic myocardium. A maximum line width change of 0.40 G was observed after 20 min of ischemia, after which either the change was insignificant or the line intensity was too low to get a precise value for the line width.

We calculated the oxygen concentration by using the observed line width data, and the values are shown in Fig. 8.

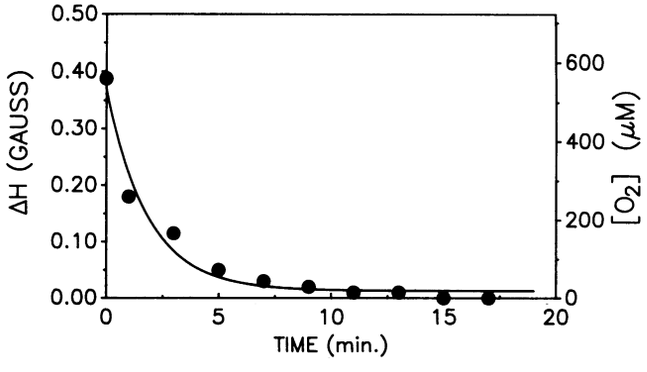

FIG. 8. Graph of myocardial oxygen concentrations in the ischemic heart as a function of the duration of ischemia. Oxygen concentration was calculated from the measured EPR linewidths. EPR measurements were made as described in Figs. 5 and 6. Kinetics of oxygen consumption were modeled with a single exponential function $k = 0.54\ min^{-1}$.

The oxygen concentration falls off very rapidly from a base value of 500 μM to 240 μM, the concentration of oxygen in air, in less than a minute, and in $\approx$10 min the value approaches zero. Fitting the data with a single exponential model gave a value of 0.54 ± 0.04 min^{-1} as the rate constant for oxygen consumption during ischemia.

DISCUSSION

Free radicals have been proposed to be important mediators of cell injury in a number of organs and tissues. Recently, it has been demonstrated that free radicals are generated in 0.1–1 μM concentrations on reperfusing ischemic tissues (10, 11). In this study, we have demonstrated that low micromolar concentrations of free radicals can be measured in large 13- to 15-mm-diameter aqueous samples and, more importantly, in whole biological organs and tissues of similar size. We have demonstrated that high sensitivity EPR measurements can be performed on these intact biological tissues by using an L-band microwave bridge with a loop-gap resonator design. This *in vivo* EPR technique was applied to measure the kinetics of free radical uptake and clearance in the perfused heart. High quality measurements were obtainable with short acquisition times enabling precise measurements and modeling. It was observed that the uptake of the TEMPO radical could be accurately modeled as a first-order exponential process with a rate constant of 0.85 min^{-1}. Clearance of the radical on termination of infusion, however, was more complex, consisting of two distinct exponential processes with different rate constants. The faster process proceeded with a rate constant of 2.2 min^{-1} and accounted for 65% of the radical loss; the slower process proceeded with a rate constant of 0.4 min^{-1}, accounting for 35% of the radical loss. In the ischemic heart, it was observed that TEMPO signal also decreased as a function of time and this process was precisely modeled as a simple first-order exponential decay with a rate constant of 0.4 min^{-1}. Since in the ischemic organ there is no washout, the loss of signal must be solely due to metabolism of the radical. The additional rapid process of radical clearance observed in the perfused heart is presumably due to vascular washout. The slower process of EPR signal decay observed in both normally perfused and ischemic hearts is probably due to enzyme reduction of the TEMPO radical. It is well known that nitroxide radicals are reduced by cells and biological tissues. Cellular reduction of nitroxide radicals has been one of the major problems encountered in applying spin-labeling and spin-trapping techniques to the study of cells (12). Lack of knowledge regarding the rate of cellular breakdown of spin-trap adducts has made it difficult to accurately determine the actual rate of radical generation in cells and tissues, since the observed concentration of spin-trap adducts or other radicals is modulated by the rate of radical generation as well as the rate of radical destruction. Thus, measurements of the rate of cellular radical metabolism in whole biological tissues are of critical importance in understanding and characterizing the mechanisms of biological free radical generation.

All biological tissues consume oxygen, and this process of oxygen consumption is of crucial importance in supplying the energy needs of cells and tissues. In the heart, 90% of the ATP generated is derived from mitochondrial oxidative phosphorylation with the energy required for the generation of ATP derived from the four-electron reduction of molecular oxygen to water (13). Incomplete reduction of O_2 results in formation of the superoxide anion radical $O_2^{-\cdot}$, hydrogen peroxide (H_2O_2), and the hydroxyl radical OH$\cdot$, which are important mediators of cellular oxidative injury. Therefore, the process of O_2 consumption is of great importance in the normal metabolism and pathology of biological organs and tissues. In this study, we have demonstrated that EPR spectroscopy can be applied to noninvasively measure cellular O_2 consumption in the isovolumic beating heart. This EPR technique can be similarly applied to other organs and tissues. Measurements of the mean oxygen concentration within the organ can be performed without mechanical perturbation of the tissue, as would occur with oxygen electrode techniques. The low (less than mM) concentrations of nitroxide radical required did not have any detectable effect on cardiac function. EPR oximetry has the unique property of targeting the specific area of distribution of the nitroxide radical used. Thus, this technique could be applied to specifically measure oxygen concentrations in different cellular locations within whole biological tissues. For example, the O_2 concentration adjacent to cell membranes could be distinguished from the concentration within the cell via the use of lipophilic radical probes that would localize within cellular membranes and hydrophilic probes that would localize in the cytosol. Thus, EPR oximetry can potentially provide information that cannot be obtained with other techniques. The technique of performing real time measurements of oxygen consumption and free radical generation or metabolism along with simultaneous measurements of contractile function is a unique and powerful method of studying free radical biology and its physiological and pathological effects on the heart. These techniques, which have been developed and applied to study the heart, can be similarly applied to other biological organs and tissues. Compared to other biological organs, the heart is relatively difficult to study with EPR spectroscopy because of its mobility and because of its change of shape as a function of the cardiac cycle. In addition, the hollow chambers of the heart decrease the efficiency of resonator filling. Therefore, in other biological tissues it should be possible to attain sensitivities equal or greater than those we have observed for the heart.

Thus, EPR spectroscopy can be applied to measure free radicals in whole biological organs and tissues. This technique is nondestructive, enabling simultaneous measurements of free radical concentrations and organ function. In addition, measurements of tissue oxygen concentrations and consumption can be simultaneously performed. This technique offers great promise in measuring and assessing the pathological effects of free radicals in whole biological organs and tissues.

This work was supported by the National Institutes of Health Grants HL-17655-13 and HL-38324 and Squibb American Heart Association Clinician Scientist Award.

1. Weisfeldt, M. L., Zweier, J. L. & Flaherty, J. T. (1988) in *Heart Disease: Clinical Update*, ed. Braunwald, E. (Saunders, Philadelphia), in press.
2. Taylor, A. E., Matalon, S. & Ward, P. (1986) *Physiology of Oxygen Radicals* (Williams & Wilkins, Baltimore).
3. Armstrong, D., Sohal, R. S., Cutler, R. G. & Slater, T. F., eds. (1984) *Aging, Free Radicals in Molecular Biology, Aging, and Disease* (Raven, New York), Vol. 27.
4. Hardy, W. N. & Whitehead, L. A. (1981) *Rev. Sci. Instrum.* **52**, 213–216.
5. Froncisz, W. & Hyde, J. S. (1982) *J. Magn. Res.* **47**, 515–521.
6. Feher, G. (1957) *Bell Syst. Tech. J.* **36**, 449–460.
7. Poole, C. P. (1967) *Electron Spin Resonance: A Comprehensive Treatise on Experimental Techniques* (Interscience, New York), pp. 523–595.
8. Freed, J. H., Leniart, D. S. & Hyde, J. S. (1967) *J. Chem. Phys.* **47**, 2762–2763.
9. Zweier, J. L. & Jacobus, W. E. (1987) *J. Biol. Chem.* **262**, 8015–8021.
10. Zweier, J. L. (1988) *J. Biol. Chem.* **263**, 1353–1357.
11. Zweier, J. L., Flaherty, J. T. & Weisfeldt, M. L. (1987) *Proc. Natl. Acad. Sci. USA* **84**, 1404–1407.
12. Samuni, A., Carmichael, A. J., Russo, A., Mitchell, J. B. & Riesz, P. (1986) *Proc. Natl. Acad. Sci. USA* **83**, 7593–7597.
13. Kobayashi, K. & Neely, J. R. (1979) *Circ. Res.* **44**, 166–175.